GLOBAL SPATIAL DISTRIBUTION OF HACK'S LAW EXPONENT ON MARS AND ITS EARLY CLIMATE. W. Luo[1], A. D. Howard[2], R. A. Craddock[3], E. A. Oliveira[4], R. S. Pires[4], [1]Northern Illinois University, DeKalb, IL, USA, [2]Planetary Science Institute, Tucson, AZ, USA, [3]Smithsonian Institution, Washington, DC, USA, [4]University of Fortaleza, Fortaleza, Ceará, Brazil

Introduction: Widespread valley networks (VNs) on Mars and other evidence point to an early warm and wet climate [e.g., 1-3]. However, ongoing debates still exist about VN's formation processes and associated climatic conditions [e.g. 4-5]. The power law relationship (Hack's Law) between the length from a locality measured along the longest channel upstream to drainage divide (L) and the area of the basin that drain to the same locality (A):

$$L = kA^h \quad (1)$$

where h is the exponent and k is a constant, can be diagnostic of different fluvial processes related to climatic conditions, with h≈0.5 for arid areas and h≈0.6 in humid regions on Earth [6-7]. Past studies of Hack's Law on Mars at local sites have produced inconclusive results [e.g., 8-9]. Here we used a parameter-free method to delineate watersheds globally on Mars based on mapped VNs and extracted their Hack's Law exponent (h). The majority of h values on Mars are similar to those in arid areas on Earth, implying similar runoff processes and arid conditions for VN formation on early Mars. Statistical analyses show that the spatial distribution of h on Mars is not random, but with a few clustered high and low values, likely controlled by local conditions (e.g., slope or structures).

Method: The standard technique to delineate watershed from DEM is to use a flow-based method that is usually implemented in GIS software. However, the flow-based method is designed for processing Earth data, and it is notoriously difficult to apply to Mars due to the disruptions and fragmentations of topography by impact cratering that post-date valley network formation. The arbitrarily chosen flow accumulation threshold can easily result in stream networks that are over- or under-extracted, and tedious human intervention is often necessary to remove spurious results [e.g., 1, 10]. Here we adapted the Invasion Percolation-Based Algorithm (IPBA), which is robust, efficient, and parameter-free [11-12], to extract watersheds draining to mapped VNs [13] on Mars. Given a regular elevation grid (Fig. 1a) and a set of sinks S (streams/valleys) (Fig. 1b), the IPBA sequentially applies the traditional Invasion Percolation algorithm over all cells of the grid, starting from a source cell (e.g., the blue cell) to form an invaded cluster (Fig. 1c). The growth dynamics iteratively add the lowest of its neighboring cells to the cluster (i.e., growing the cluster by invading the surrounding cells; the invaded cell becomes blue, Fig. 1c, see Fig. 1a for elevation). The invaded cluster grows until it reaches a sink cell (or a cell that was once part of an invaded cluster in previous IPBA iterations) and the invaded cluster is labeled with the ID of the sink cell (or the ID of the cluster already labeled, e.g., "3" in Fig. 1c). The clusters draining to the same VN/stream are grouped to form the watershed of that VN/stream (same color in Fig. 1d). Finally, the contact edge between different watersheds (different colors) is then marked as the watershed boundary between them (Fig. 1e). The python code for this version of IPBA is available on GitHub (https://github.com/erneson/IPBA).

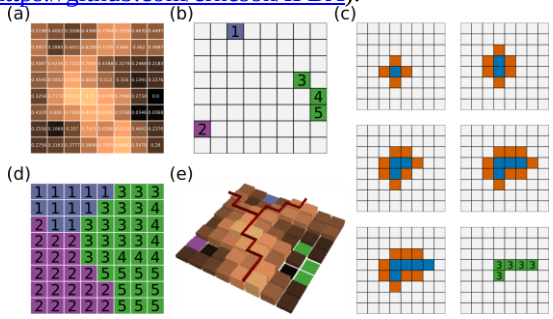

Figure 1. Illustration of IPBA. See text for details.

To obtain h of each watershed, we first clipped the DEM using the watershed boundary derived from IPBA, one watershed at a time, then used the flow-based method to extract A and L in Eq. (1) using the flow accumulation and flow length tools, respectively, in ArcGIS Pro. Next, the optimize.curve_fit function in SciPy was used to fit the power law relationship to obtain the exponent h in Eq. (1).

Results: *Terrestrial.* To provide context and aid in interpreting our results for Mars, we extracted h for the conterminous US as described above. Our results, although slightly different in values, are generally consistent with those of [7] (Table 1). The h values are generally higher in humid regions (0.54) than those in arid ones (0.50) (Table 1, Fig. 2a & 2b). Statistic t-test show that the difference of Hack's law exponents between the humid and arid regions are highly statistically significant ($p<0.0001$, one-tail). Spatial autocorrelation analysis (Global Moran's I) of h over conterminous US generated a Moran's Index of 0.2297, a z-score of 7.733 and a p-value of <0.0001, which means that the distribution is highly clustered and the null hypothesis of random distribution can be safely rejected. This makes sense, because we know on Earth fluvial processes are primarily responsible for the formation of drainage systems. Optimized Hot Spot Analysis (not shown) reveals hotspots at the Wyoming-

Dakota border around the Black Hills area and in the area transitioning from Great Plains to Central Lowland area. The cold spots are generally located at the Basin and Range Province and Colorado Plateau, a generally very arid region. The hotspots (high *h* values) are likely caused by fluvial erosion that elongated the watershed in the downslope direction. The cold spots (low *h* values) are related to the arid climate and/or structure control of basin and range.

Mars. Fig. 3a shows the spatial distribution of *h* of the 2562 watersheds on Mars that are not on the edge of the DEM grid, because those on the edge have artificial straight boundaries, which could result in inaccurate *h*. Fig. 3b shows the histogram of *h* of the 2406 watersheds (basins with poor fitting for *h* ($r^2 < 0.75$) excluded). The histogram is roughly normally distributed, ranging from 0.28 (min) to 2.1 (max) (see also Table 1). The mean *h* value of these basins (n=2406) is 0.50, which is slightly lower than the mean value of 0.54 for the US, and majority of values are between 0.4 and 0.6. The mean Martian value is closest to that of the mean values of cold spots (0.48) and arid area (0.50) in the US (see Table 1). Spatial autocorrelation analysis (Global Moran's I) of *h* on Mars with the same null hypothesis (that the spatial distribution of *h* is random) generated a Moran's Index of 0.050, a z-score of 10.891089 and p-value of <0.0001, which also indicates that the spatial distribution is clustered and the null hypothesis can be safely rejected. This result suggests that the processes responsible for the VN formation on Mars were not random.

Optimized Hot Spot Analysis (Getis-Ord Gi*) reveals 8 hotspots and 1 cold spot (not shown). Overall, the hotspot areas are related to the underlying topography and appear to be influenced by planar surfaces of volcanic lava flows and structures. The VNs in cold spot area are poorly developed or modified.

The statistics of *h* values of all basins and different categories of hot/cold spots are summarized in Table 1. The majority of the Martian basins are in the non-hot/cold spots category with mean and median h values of 0.49, similar to those of arid area and cold spots on in the US (0.48-0.5) (Table 1). The standard deviation values of h on Mars in all categories are small and comparable with their terrestrial counterparts (Tables 1). One signature of *h* value for fluvial systems on Earth is that it clusters tightly around 0.5-0.6. The fact that there is wide spatial distribution of *h* on Mars with value similar to arid climate on Earth and with small standard deviation comparable to terrestrial values suggest Martian VNs were likely formed in arid climate by fluvial runoff processes in arid climate. This conclusion is also supported by other recent studies [e.g., 14] and the spatial autocorrelation analysis result that the processes responsible for VN formation were not random.

Acknowledgments: NAASA MDAP (80NSSC21K1087 & 80NSSC17K0454) and Edson Queiroz Foundation (to EO and RP).

References: [1] Ansan V & Mangold N (2013) JGR, 118(9), 1873–1894. [2] Craddock, R. A. & Howard, A. D. (2002) JGR, 107(E11). [3] Luo W. & Stepinski, T. F. (2009) JGR, 114. [4] Fastook, J. L. & Head J. W. (2015) PSS, 106, 82–98. [5] Grau Galofre, A. et al. (2020) Nat. Geosci. 13(10), 663–668. [6] Hack J. T. (1957) USGS. [7] Yi R. S. et al. (2018) Proc. Royal Soc A., 474(2215), 20180081. [8] Som S. M. et al. (2009) JGR, 114(E2). [9] Penido J. C. et al. (2013) PSS, 75, 105–116. [10] Mest, S. C. et al. (2010) JGR, 115(E9). [11] Fehr E. et al. (2009). J. Stat Mech, 2009(09), P09007. [12] Oliveira E. A. et al. Sci. Rep., 9(1), 9845. [13] Matsubara Y. et al. JGR, 118(6), 1365–1387. [14] Cang X & Luo W (2019) EPSL, 526, 115768.

Table 1 Statistics of *h* for conterminous US and Mars

		Categories	n	Mean	Standard deviation
Earth (US)	Basic statistics	All	308	0.54	0.079
		Arid[1]	42	0.50	0.053
		Humid[1]	160	0.54	0.077
	Hotspot analysis[2]	Included (r^2≥0.75)	302	0.54	0.073
		Cold Spots	10	0.48	0.053
		Hot Spots	22	0.64	0.124
		Non- hot/cold spots	270	0.54	0.062
Mars	Basic statistics	All	2562	0.49	0.086
	Hotspot analysis[2]	Included (r^2≥0.75)	2406	0.50	0.077
		Cold Spots	12	0.44	0.031
		Hot Spots	93	0.57	0.090
		Non-hot/cold spots	2301	0.49	0.075

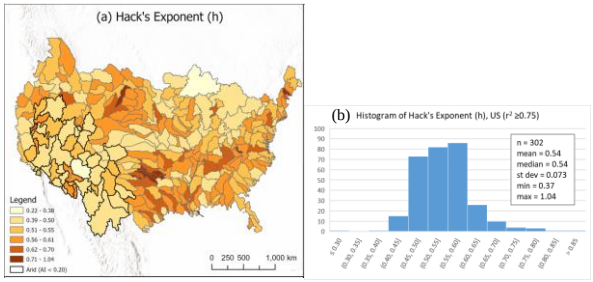

Fig 2 (a) *h* for US (b) Histogram of *h* for US.

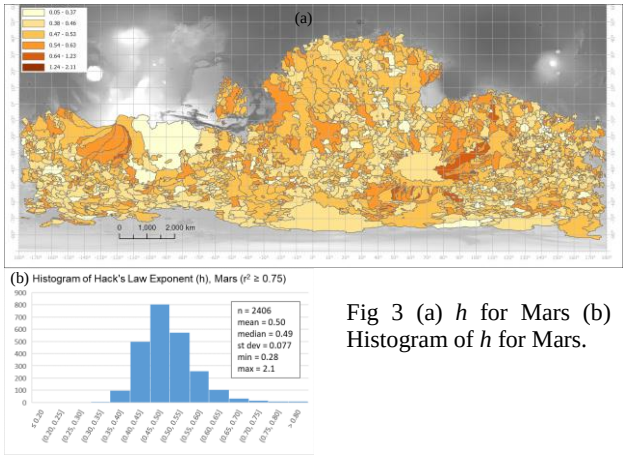

Fig 3 (a) *h* for Mars (b) Histogram of *h* for Mars.